JOURNAL OF CATALYSIS **168,** 463–470 (1997)
ARTICLE NO. CA971638

Tantalum Pillared Montmorillonite

II. Acidic and Catalytic Properties

G. Guiu and P. Grange

Catalyse et Chimie des Matériaux divisés, Université Catholique de Louvain, Place Croix du Sud 2/17, 1348 Louvain-la-Neuve, Belgium

Received October 17, 1996; revised January 15, 1997; accepted January 15, 1997

The acidic and catalytic properties of a series of Ta-PILCs synthesized with a different initial tantalum content were characterized by adsorption of gaseous probe molecules (TPD of ammonia and FTIR spectra of absorbed pyridine) and by the test reaction of 1-butanol dehydration. A large increase of acidity was noted in Ta-PILCs compared to Na-montmorillonite or tantalum oxide. Cross-linking pillars and silica layers of the clay induce stronger Lewis and new Brønsted sites. The lack of basic sites formation is evidenced by the dehydration of 1-butanol to butene selectivity (100%). The incorporation of the tantalum oxide between the montmorillonite sheets produce, within Ta-PILC, acid centers of the same nature as observed for the silicon–tantalum mixed oxides.

INTRODUCTION

Clays (1), silica-aluminas (2), and zeolites (3, 4) are widely used as catalysts in a large number of acid reactions. Their properties, as solid acids, depend on the number, nature (Lewis or Brønsted), and strength of their acid sites existing on the surface.

In the case of montmorillonite, a clay which belongs to the group of the smectites, the origin of its acidity is well established. In fact, it is considered that Brønsted acidity essentially results from the dissociation of water molecules in the hydration shell of the interlayering exchangeable cations (5). On the other hand, Lewis acidity results from the low coordination of aluminium atoms at crystal edges of the clay sheet (6).

The pillared clays are synthesized by intercalation of voluminous polyoxocations in the interlayer space of a swelling clay. The introduction of these polyoxocations in the interlayer space and the later calcination of the intercalated clays led to a new type of solid acid, which has been assimilated with bidimensional molecular sieves (7, 8).

There is a general agreement on the existence of two types of acid sites: Lewis and Brønsted, on the pillared clays surface (9, 10). It is widely admitted that pillars are the source of the Lewis acidity improvement observed for all the pillared clays. After calcination, the pillar precursors, symbolized generally as $M_xO_y(OH)_z$, are transformed into metal oxides. The contribution of the pillars to the acidity of pillared clays should therefore be mainly of the Lewis type. The Brønsted acidity observed in pillared clays is usually lower than the Lewis acidity.

The number and strength of the acid sites created by the pillars mainly depend on the metal chosen as precursor. Nowadays, aluminium, titanium, and zirconium are the most studied metals (11, 12). Once the metal precursor is chosen, the synthesis experimental conditions and the nature of the clay will be those which define the pillared clay performances.

The first objective of this paper is to estimate the Ta-PILC acidic and catalytic properties which, as mentioned above, include the determination of the quantity, nature (Lewis and/or Brønsted), and strength of the acid sites.

The evaluation of the acidic properties of tantalum pillared clays has been carried out upon the series of Ta-PILC, whose physicochemical characterization has been presented in the first paper of this series (13). The study of the properties of these Ta-PILCs synthesized with different initial tantalum contents has allowed us to analyze the influence of the quantity of tantalum incorporated into the clays on the pillared clay performances.

The second objective of this paper is to better understand the origin of the acidic properties of Ta-PILCs. For this purpose, we have tried to simulate the interaction as it could happen between the tantalum oxide pillars and the montmorillonite tetrahedral silicon layer through a model system where the Si–O–Ta interaction exists. The chosen model system has been silicon–tantalum mixed oxides (14, 15). The comparative analysis of acidic properties and catalytic performances of both systems allows one to better understand the type of interaction and the nature of the acid sites existing within the Ta-PILC.

METHODS

A detailed description of acid surface properties would include the determination of the amount, nature (Lewis or

0021-9517/97 $25.00

Brønsted), and strength of the acid and base sites. In seeking this information, two methods were used: (i) adsorption of gaseous probe molecules (TPD of ammonia and FTIR of adsorbed pyridine) (10, 16) and (ii) catalytic activity in a model reaction (1-butanol dehydration) (17). Earlier studies have brought to the fore the utility of 1-butanol dehydration as a test reaction for characterizing the acid–base properties of catalysts. Indeed, reaction products and their relative proportion supply very interesting information about the nature of active sites on the catalysts surface.

NH_3 TPD analyses were carried out using samples calcined at 500°C. Prior to the ammonia adsorption, samples were treated at atmospheric pressure in a flow of helium at 400°C for 4 h. Ammonia adsorption was carried out at 120°C for 15 min. The physisorbed ammonia was eliminated by maintaining the samples in a flow of helium at the adsorption temperature for 1 h.

The chemisorbed ammonia desorption was carried out in two steps. The evaluation of the ammonia desorbed at each step allowed the arbitrary division in more (400–700°C) and less (120–400°C) strongly chemisorbed ammonia. In a first step, the linear temperature increase from 120 to 400°C, at a rate of 4°C/min, results in the desorption of a share of the chemisorbed ammonia. The ammonia desorbed with increase in temperature was continuously recorded by a thermal conductivity detector. In addition, desorbed ammonia was collected in a boric acid solution and titrated with sulfuric acid according to the Kjeldahl method (18).

In a second step, the temperature increase from 400 to 700°C, at a rate of 4°C/min, leads to the desorption of the most strongly chemisorbed ammonia. The quantity of ammonia released in this interval was measured by titration of a boric acid solution.

Pyridine FTIR spectra were recorded using a Brucker FT 88 spectrometer. Samples were calcined at 500°C before analysis. In preparation for pyridine adsorption, samples were pressed into self-supported disks, placed in an IR cell, and treated under vacuum (10^{-6} Torr) at 400°C for 4 h. After cooling to room temperature, spectrum (a) was recorded. The samples were then exposed to pyridine vapor for 5 min. After evacuation (5×10^{-5} Torr) at room temperature for 1 h, spectrum (b) was recorded. Spectra (c), (d), and (e) correspond to subsequent successive outgassing of samples at 150, 250, and 400°C, respectively.

The test reaction, 1-butanol dehydration, was carried out at atmospheric pressure in a fixed-bed reactor (i.d. 4 mm). Before reaction, the catalysts were sieved and the particle size fraction of 100–200 μm was used. The catalyst mass was 60 mg and the corresponding bed height was adjusted to 14 mm, by adding 100- to 200-μm glass balls. Catalyst activation was performed in helium flow at reaction temperature for 1 h. Helium, the carrier gas, was used to entrain 1-butanol into the vapor phase from a saturator held at 53°C (5.5 KP butanol partial pressure). This helium/1-butanol gas reaction mixture passed through the reactor at a rate of 60 ml/min flow (LHSV = 9.8 h^{-1}).

Depending on the nature of the catalyst active sites, the 1-butanol dehydration products are butyraldehyde, dibutylether, and 1-butene. Simultaneously, under the reaction conditions, the 1-butene formed isomerizes to *cis*- and *trans*-2-butene.

To prevent 1-butanol, butyraldehyde, and dibutylether condensation, all lines from the saturator to the chromatograph were heated to 100°C. The dehydration products and 1-butanol were analyzed by gas chromatography using a Shimadsu GC-8A chromatograph equipped with a thermal conductivity detector. A 20% Reoflex/400Embacel column, 2 m long, was used to separate and quantify the 1-butanol and the dehydration products, butyraldehyde and dibutylether. 1-Butene and the isomerization products, *cis*- and *trans*-2-butene, were analyzed by a 2-m Octane/Porasil column. Both columns operated isothermally at 60°C and the carrier gas was helium.

RESULTS

Catalyst Preparation

The preparation procedure has been reported previously (13). Let us just recall that the starting material, a Kunimine Industry Co. Ltd. Na-montmorillonite, was dispersed in water and aged for at least 1 month before pillaring. The tantalum pillaring solution was prepared by careful control of the hydrolysis of a tantalum alkoxide precursor, $Ta(OC_2H_5)_5$, in an ethanolic solution. Then the Ta/clay ratio in the suspension was adjusted in order to prepare a series of Ta-PILC with variable tantalum content. Details of the micromoles of Ta per gram of clay ratio for the different samples are given in Table 1. The obtained suspension was washed, dried, and finally calcined, in different steps, until it reached 500°C.

TABLE 1

Samples Nomenclature and Initial Tantalum Content (mmol Ta/g of clay) for this Series of Ta-PILC

Samples	Ta/clay ratio (mmol/g)
PILC-[Ta]1	0.77
PILC-[Ta]2	1.54
PILC-[Ta]3	2.31
PILC-[Ta]4	3.08
PILC-[Ta]5	3.86
PILC-[Ta]6	4.63
PILC-[Ta]7	5.40
PILC-[Ta]8	6.17

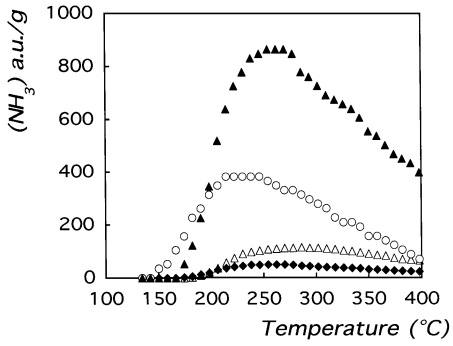

FIG. 1. Recorded response of desorbed NH_3 (arbitrary units)/g of catalysts: (△) tantalum oxide, (◆) Na-montmorillonite, (○) PILC-[Ta]3, and PILC-[Ta]8 (▲) as a function of temperature.

TPD of Ammonia

Figure 1 illustrates the profiles of desorbed ammonia ((NH_3)a.u. per gram of catalysts) as a function of the desorption temperature for a representative selection of pillared clays belonging to this series of Ta-PILCs, as well as for the starting materials, Na-montmorillonite and tantalum oxide.

Ta-PILC ammonia desorption spectra are quite similar and they typically consist of a very broad band. The NH_3 desorption signal starts at approximately 170°C and at 400°C, the higher limit of this first temperature interval, the profiles do not return to their baseline indicating that the ammonia desorption continues beyond this temperature. All the Ta-PILC desorption spectra present a maximum between 225 and 275°C.

Table 2 reports the amount of chemisorbed NH_3 desorbed from Ta-PILCs as well as from the starting materials for the two intervals of temperature analyzed. Figure 1 and Table 2 emphasize that the total acidity increases on Ta-PILCs compared to Na-montmorillonite or even tantalum oxide. Besides, the quantity of ammonia desorbed in the first temperature interval, from 120 to 400°C, is slightly enhanced with the initial tantalum content, except for the PILC-[Ta]5 sample (Table 2). The ammonia more strongly chemisorbed, which is desorbed between 400 and 700°C, remains almost constant for all the samples of this series. However, it is important to note that, as the temperature reached through this second desorption interval (700°C) is higher than the calcination temperature (500°C), the values obtained in this way must be carefully considered.

TABLE 2

Chemisorbed Ammonia Desorbed from Tantalum Oxide, Na-Montmorillonite, and Ta-PILCs, Precalcined at 500°C

Sample	Quantity of NH_3 desorbed (μmol·g^{-1})		
	120–400°C	400–700°C	120–700°C
Na-montmorillonite	40	—	40
Ta_2O_5	175	—	175
PILC-[Ta]3	583	100	683
PILC-[Ta]4	590	101	691
PILC-[Ta]5	490	115	605
PILC-[Ta]6	602	110	712
PILC-[Ta]8	638	104	742

FTIR Spectra of Adsorbed Pyridine

The spectroscopic study of adsorbed bases such as pyridine is a useful tool for the characterization of the nature of pillared clays surface acidity (19–22).

Figure 2 illustrates the spectra of adsorbed pyridine on tantalum oxide, Na-montmorillonite, and Ta-PILCs (PILC-[Ta]6), evacuated at various temperatures. The evolution of FTIR spectra of adsorbed pyridine is very similar for all the Ta-PILCs studied; therefore, in Fig. 2 only one representative evolution is shown.

As can be seen in Fig. 2, increasing the outgassing temperature results in a reduction of the intensity of all absorption bands. Spectra b, pyridine adsorbed after outgassing at room temperature, show in addition to their characteristic vibration modes, the band of physisorbed pyridine at approximately 1600 cm^{-1}.

Figure 2, spectrum d, pyridine adsorbed on tantalum pillared clays after outgassing at 200°C, exhibits Brønsted BPy bands at 1491, 1547, 1578, and 1640 cm^{-1} and Lewis acid bands at 1451, 1491, 1576, 1614, and 1625 cm^{-1}. Sodium montmorillonite and tantalum oxide evacuated at 200°C, after adsorption of pyridine, present only Lewis LPY bands.

Bands typical of Brønsted acidity on Ta-PILCs are eliminated after outgassing above 200°C. However, characteristic Lewis bands are still observed even after outgassing at 400°C, see Fig. 2. With regard to Na-montmorillonite and Ta_2O_5, evacuation at 200°C almost completely removes pyridine adsorbed on Lewis acid sites.

Table 3 reports the wavenumbers of the pyridine coordinated to Lewis acid sites on Ta-PILCs, Na-montmorillonite,

TABLE 3

Characteristic Wavenumbers of Pyridine Coordinated to Na-Montmorillonite, Ta-PILCs, and Ta_2O_5 after Outgassing at Various Temperatures

		Na-montmorillonite		Ta-PILC		Ta_2O_5	
Type	Band	100°C	200°C	200°C	300°C	150°C	250°C
LPY	19b	1444	1445	1451	1451	1448	—
		—	—	—	1459	—	—
	19a	1491	1491	1491	1493	1489	—
	8b	1578	—	1576	—	1577	—
	8a	1602	—	1614	1615	1611	—
		1621	1624	1625	1625	—	—

Note.—, After outgassing at the pointed out temperature this vibration band is not present anymore.

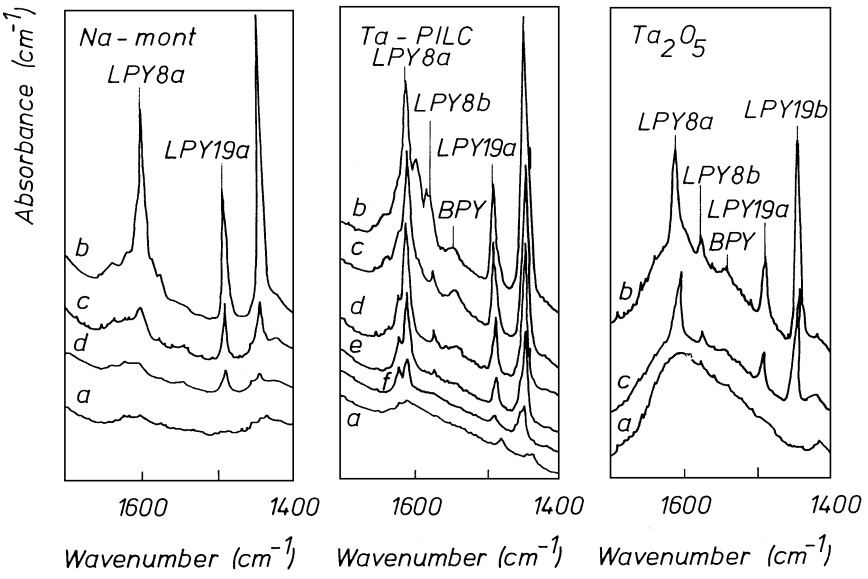

FIG. 2. FTIR spectra of pyridine adsorbed on tantalum oxide, Na-montmorillonite, and Ta-PILCs (PILC-[Ta]6). Spectra before pyridine adsorption (a) and sample exposed to pyridine and outgassed at room temperature (b), 100°C (c), 200°C (d), 300°C (e), and 400°C (f).

and tantalum oxide after outgassing at different temperatures. At a given temperature the wavenumbers of pyridine adsorbed upon Lewis acid sites remain always higher for Ta-PILCs than for tantalum oxide or Na-montmorillonite.

As can be seen in Table 3, tantalum oxide calcined at 500°C and evacuated at 150°C presents only one characteristic LPY 8a band at 1611 cm^{-1}. However, Ta-PILCs exhibit a (LPY 8) band split into two: $(LPY\ 8a)_1$ at 1625 cm^{-1} and $(LPY\ 8a)_2$ at 1615 cm^{-1}. The existence of two characteristic wavenumbers is clearly observed for the LPY 8a absorption band. This band is the one usually presenting the largest shifts. However, after outgassing the Ta-PILCs above 300°C, a new shoulder is also observed for LPY 19b.

A semiquantitative analysis of the Lewis and Brønsted acid sites was carried out using the developed IR band intensities. The intensity of the acid bands was calculated on the basis of the band integral area (a.u.) and wafer density (mg/cm^2). Calculated intensities of Brønsted (BPY = 1545 cm^{-1}) and Lewis (LPY = 1450 cm^{-1}) acid bands after outgassing at 200°C are given in Table 4.

The third column of this table presents the ratio of LPY band integral area to BPY band integral area. This value can be considered as the ratio between Lewis and Brønsted acid sites multiplied by a constant ((L/B) × cte), cte = LPy molar extinction coefficient/BPY molar extinction coefficient.

The intensity of the LPY band is remarkably enhanced in Ta-PILCs compared to tantalum oxide. Lewis acidity is predominant in all the tantalum pillared clays. The ratio of LPY to BPY band integral areas increases with the tantalum content. The BPY band integral area remains roughly constant for this series of Ta-PILCs, except PILC-[Ta]5. The increase in I(Lewis)/I(Brønsted) value can therefore be entirely assigned to a rise in the density of Lewis acid sites.

1-Butanol Dehydration Test Reaction

Table 5 presents the results of the 1-butanol dehydration reaction (conversion and selectivity at steady state, after 2 h reaction using catalysts calcined at 500°C). Selectivity for produced butenes and dibutylether is defined as the molar ratio of each product to 1-butanol converted. On tantalum oxide and tantalum pillared clays, no deactivation was observed even after 5 h on stream.

Table 5 gives evidence of the great improvement in 1-butanol conversion for Ta-PILCs compared to the starting materials, Ta_2O_5 and Na-montmorillonite.

TABLE 4

Calculated Intensities of Lewis and Brønsted Acid Bands as Well as the I(Lewis)/I(Brønsted) Ratio for Na-Montmorillonite, Ta-PILCs, and Ta_2O_5 after Outgassing at 200°C

Sample	I(Lewis) (1450 cm^{-1}) (a.u. g^{-1})	I(Brønsted) (1545 cm^{-1}) (a.u. g^{-1})	I(Lewis)/ I(Brønsted)
Na-montmorillonite	9	0	—
Ta_2O_5	15	0	—
PILC-[Ta]2	149	32	4.65
PILC-[Ta]3	171	32	5.34
PILC-[Ta]4	221	36	6.14
PILC-[Ta]5	111	18	6.17
PILC-[Ta]6	213	33	6.45
PILC-[Ta]8	296	41	7.22

TABLE 5

Test Results of 1-Butanol Dehydration Using Tantalum Oxide, Na-Montmorillonite and Ta-PILCs, at Steady State and after 2 h Reaction

Sample	Reaction temperature (°C)	Butanol conversion (%)	Selectivity			
			1-Butene	*cis*-2-Butene	*trans*-2-Butene	DBE
Na-montmorillonite	250	1	8.2	6.1	4.1	81.6
	300	3	25.0	28.6	21.4	65.4
Ta_2O_5	250	1	63	22	16	0
	300	7	61	24	15	0
PILC-[Ta]2	250	15	25.9	36.4	37.7	≤0.1
	300	26	33.9	35.3	30.8	≤0.1
PILC-[Ta]3	250	15	28.0	36.2	35.8	≤0.1
	300	35	34.1	35.8	36.1	≤0.1
PILC-[Ta]4	250	18	27.6	37.6	34.8	≤0.1
	300	46	31.3	37.9	30.8	≤0.1
PILC-[Ta]5	250	17	31.7	36.3	32.0	≤0.1
	300	45	32.9	37.0	30.1	≤0.1
PILC-[Ta]6	250	15	28.5	37.8	33.7	≤0.1
	300	41	31.8	37.8	30.4	≤0.1
PILC-[Ta]8	250	25	29.4	38.0	32.6	≤0.1
	300	63	31.4	38.4	30.2	≤0.1

Tantalum pillared clays and tantalum oxide present almost the same dehydration product yields. Indeed, in the range of temperatures tested, the main dehydration product over Ta_2O_5 and Ta-PILC is 1-butene, 100% selectivity. With regard to dibutylether, this product is not observed when Ta_2O_5 is used as catalyst and for Ta-PILCs the integral of its signal never represents more than 0.1% of initial 1-butanol. Concerning butyraldehyde, this dehydration product is never detected in the products stream.

In addition, one can also find from Table 5 that the Na-montmorillonite shows a much lower conversion than Ta_2O_5 or Ta-PILCs and a completely different dehydration product yield. In this case dibutylether appears to be the main dehydration product and the 1-butene selectivity is reduced to 20%.

As pointed above, under the reaction conditions, 1-butene produced is partially isomerised to *cis*- and *trans*-2-butene. In the 250–300°C reaction temperature range, isomerization of 1-butene remains roughly constant and equal to 67–74% for all Ta-PILCs. On the other hand, the results of 1-butene isomerization over the Ta_2O_5 catalyst reveal a much lower order of conversion, i.e., 34–38%. On these catalysts, the *cis*-/*trans*-2-butene ratio in the isomerization products is 1.0–1.3 and 1.5 for Ta-PILC and Ta_2O_5, respectively.

DISCUSSION

Probe Molecules Adsorption

From the quantitative analysis of adsorbed ammonia and from the FTIR spectra of adsorbed pyridine (Tables 2 and 4, respectively), a large increase of acidity is noted in Ta-PILC compared to Na-montmorillonite or tantalum oxide. This increase is certainly due to the intercalation of tantalum pillars between the montmorillonite layers. In addition, the quantitative analysis of adsorbed ammonia points out that the number of acid sites tends to rise with the tantalum initial content.

The FTIR spectra of adsorbed pyridine shows the existence of two types of acid sites, Lewis and Brønsted, on the surface of the tantalum pillared clays. Sodium montmorillonite and tantalum oxide evacuated after adsorption of pyridine present only Lewis LPy bands. This implies the existence, on Ta-PILCs, of Brønsted acid sites absent on the starting materials.

The ratio between LPy and BPy integral areas rises with tantalum content. Besides the BPy band, integral area remains roughly constant for this series. These observations agree with the widely admitted hypothesis that, after calcination, pillars contribution to pillared clays acidity is mainly Lewis type. As can be seen in Fig. 3, the increase in the Lewis acidity of Ta-PILCs is directly correlated with the pillared clays tantalum final content, calculated by atomic absorption spectrophotometry (13).

The strength of Lewis acid sites to which pyridine is coordinated, has been analyzed according to the LPy 8a band wavenumber. The LPy 8a band of coordinated pyridine shifts from 1610 to 1640 cm^{-1} depending on the pyridine–Lewis center interaction strength.

The analysis of the pyridine adsorbed on Lewis acid sites shows that for Ta-PILCs these bands are split into two. These two bands are well differentiated for (LPy 8a)

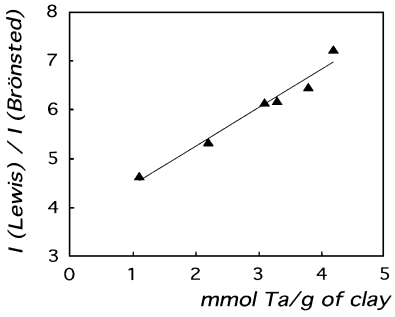

FIG. 3. Recorded I(Lewis)/I(Brønsted) ratio as a function of the Ta-PILC final tantalum content, estimated by atomic absorption spectrophotometry.

vibration mode: $(LPy\ 8a)_1 = 1624\ cm^{-1}$ and $(LPy\ 8a)_2 = 1615\ cm^{-1}$. The observation of two bands for the same vibration mode implies the existence of two different types of Lewis acid sites on tantalum pillared clays.

As a matter of fact, the $(LPy\ 8a)_1$ band $= 1624\ cm^{-1}$ can be associated with the $(LPy\ 8a) = 1625\ cm^{-1}$ of Na-montmorillonite, namely the origin of these Lewis acid sites would be the low coordination of aluminium atoms at crystal edges of the clay sheets.

On the other hand, the second (LPY 8a) band on Ta-PILCs, $(LPy\ 8a)_2$ can be associated with the tantalum intercalated in the interlayer space of the clay. However, the wavenumber at which the $(LPy\ 8a)_2$ band appears in Ta-PILCs, 1615 cm^{-1}, is meaningfully higher than in tantalum oxide, 1611 cm^{-1}. In the same way, the temperature required to eliminate the adsorbed pyridine from these Lewis acid sites is much lower in Ta_2O_5 (250°C) than in Ta-PILCs (still present at 400°C).

From all the facts described above, the probe molecules adsorption measurements underline that the Ta-PILC's performances: (i) amount and (ii) nature of acid sites cannot be considered as a result of the simple addition of Na-montmorillonite and tantalum oxide acidic properties.

Test Reaction

In agreement with pyridine FTIR and ammonia TPD, 1-butanol dehydration shows that Ta-PILCs possess a greater number of acid sites than Ta_2O_5 or Na-montmorillonite.

1-Butanol dehydration can take place by elimination reaction mechanisms E1, E2, or E1cB (cB, conjugate base). The accepted mechanism for 1-butanol dehydration using solid catalysts such as alumina and silica–alumina is of type E2. This is a one-step mechanism where the alcohol OH group is eliminated by an acid function and a proton in the β position is eliminated by a basic site. Therefore, 1-butanol dehydration by E2 type elimination reaction requires the existence of acid and basic sites on the catalyst surface.

From alumina and silica–alumina, the possibility of E2 elimination, as reaction mechanism, is supported by the simultaneous existence of butene and dibutylether as 1-butanol dehydration products. The formation of dibutylether from 1-butanol requires the existence of both acid and basic sites on the catalyst surface.

In the temperature range studied, for tantalum oxide, the selectivity to butenes is 100%, i.e., neither butyraldehyde nor dibutylether are formed. This indicates that for Ta_2O_5 1-butanol dehydration takes place via the formation of a carbonium ion and implies an E1 type mechanism (23). That means that the catalytic active sites under the reaction conditions studied are the acid sites. Basic sites do not take part in the elimination reaction.

For Ta-PILC the selectivity to butenes is nearly 100%. Butyraldehyde is not formed and the maximum percentage of 1-butanol transformed on dibutylether is very low, i.e., 0.1% at 225°C. This percentage decreases with the reaction temperature. That is, the catalytic active sites on Ta-PILCs are mainly acid sites. Moreover, as illustrated in Fig. 4, the percentage of 1-butanol converted on each sample of this series is directly correlated with the density of Lewis acid sites (pillars density) calculated by FTIR spectra of adsorbed pyridine.

As described above, the production of dibutylether requires the existence of both acid and basic sites. The origin of the basic sites on Ta-PILCs can certainly be associated with the montmorillonite sheet edges. Indeed, two tetrahedral (T) layers of polymerised SiO_4 units and one octahedral (O) layer polymerized of Al_2O_3 are the basic building blocks of the montmorillonite. These layers condense together forming a T–O–T sandwich structure. The surface at the crystal edges of the montmorillonite corresponds then quite accurately to the silica–alumina surfaces. Moreover, silica–aluminas are solids well known for presenting a large number of basic sites on their surfaces. Therefore, as for silica–aluminas, the basic sites on Ta-PILC will be oxygen ions or hydroxyl groups located at the clay sheet edges.

This hypothesis is supported by the fact that dibutylether is not detected for 1-butanol dehydration on Ta_2O_5. On the other hand, dbutylether is produced when Na-montmorillonite is used as catalyst. Besides, the almost negligible amount of 1-butanol transformed on dibutylether

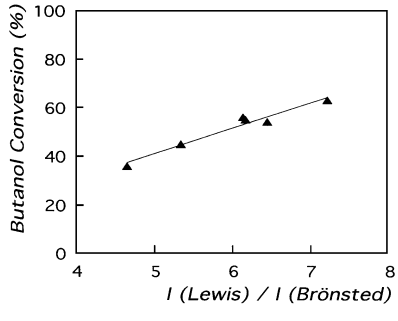

FIG. 4. Butanol converted (%) as a function of the recorded I(Lewis)/I(Brønsted) ratio.

indicates the very low extension of the surface responsible for this transformation. This agrees with the small proportion of the total surface area effectively developed by the clay sheet edges.

Under the reaction conditions employed, 1-butene obtained from 1-butanol dehydration is partially isomerized to *cis*- and *trans*-2-butene. Many studies have already been carried out concerning 1-butene isomerization as a test reaction to determine the nature of active centers on the catalyst surface. In fact, the isomerization of 1-butene to 2-butene takes place by a hydrogen transfer mechanism. This hydrogen may come from a Brønsted acid site or from a neighboring carbon. The latter implies the existence of basic functions. The value of *cis*-/*trans*-2-butene ratio in the isomerization products depends on the origin of the transferred hydrogen. It has been shown that for solids which possess Brønsted acid sites, the *cis*-/*trans*-2-butene ratio value is characteristically 1.5 (24–27), whereas on solids where the isomerization occurs by basic sites this ratio value is significantly higher (28, 29). The *cis*-/*trans*-2-butene ratio obtained for the isomerization of 1-butene for Ta-PILCs tested is approximately 1.2 (1.0–1.3). This ratio is close to the one obtained for Ta_2O_5 (1.4–1.5) and implies then that the isomerization by acid catalysis via a butylcarbonium as ion intermediate.

For Ta-PILCs, the conversion of 1-butene to *cis*- and *trans*-2-butene is constant and equal to 67–74%, whereas tantalum oxide gives a conversion of 34–38%. Since with these solids 1-butanol dehydration proceeds mainly via an E1 mechanism, that is acid catalysis (Brønsted and Lewis), and 1-butene isomerization is catalyzed by Brønsted acid sites, then the Brønsted/Lewis ratio must be higher in Ta-PILCs than in tantalum oxide. This observation corroborates the FTIR spectra of adsorbed pyridine results.

Silicon–Tantalum Mixed Oxides and Tantalum Pillared Clays Comparative Analyses

Through the analysis of acidic and catalytic properties of Ta-PILCs a remarkable enhancement of pillared clays performances compared to Na-montmorillonite or tantalum oxide has been observed. Otherwise, the nature of Ta-PILCs acid sites cannot be simply explained as having its origin in the starting materials. In order to seek the origin of the acidity present on Ta-PILCs several concepts about pillared clays must be recalled.

Preparation of PILCs molecular sieves involves the ion exchange of voluminous polyoxocation species in the interlayer space of a swelling clay. Upon calcination below the dehydroxylation temperature of the clay lattice, clay sheets are cross-linked by the pillars. This cross-linking immobilizes the polycation species in the interlayer space, thereby producing a permanently propped porous structure.

That some kind of cross-linking occurs between the temperature at which pillars dehydroxylate and the temperature at which the clay lattice dehydroxylates is supported by several experimental observations: (i) After calcining, between 400 and 500°C, the pillars are no longer exchangeable. (ii) The d(001) spacing does not change when the calcined pillared clays are redispersed. In other words, upon thermal treatment swelling properties of the smectite are lost. The hydration energy of cations is not able to overcome the interactions existing between the clay sheets and the pillars anylonger. This is true for all pillared clays.

However, the generic term "cross-linking" may cover different processes depending on the nature of the starting clay (30). Two kinds of cross-linking mechanisms appear possible. (i) In the case where the clay lattice charge is more localized (beidellite, fluorohectorite) cross-linking involves the rearrangement of chemical bonds and, eventually, the inversion of tetrahedral elements (either Si^{IV} or Al^{IV}) toward the gallery. (ii) In other cases (montmorillonite), cross-linking seems to result from cohesive forces bringing dehydrated and dehydroxylated pillars into contact with the clays sheets. In fact, for this kind of clays, the nature of the cross-linking process is not yet fully understood.

Even if the studies carried out to this very day do not bring any conclusive evidence about the nature of the interaction responsible for the cross-linking mechanism in pillared montmorillonites, it seems clear that this interaction should take place between the elements of the pillar and the clay tetrahedral layer. Therefore, for the tantalum pillared montmorillonite this interaction would be produced between the tantalum oxide and the tetrahedral layer of the montmorillonite: (SiO_2).

The acidic and catalytic comparative analyses of Ta-PILCs with a model system where the Si–O–Ta interaction exists have allowed us to better understand the contribution of the pillar–clay linkage to the acidity enhancement as well as to the origin of the nature of the acid sites present on the tantalum pillared clays. The chosen model system has been silicon–tantalum mixed oxides.

The acidic and catalytic properties of SiO_2–Ta_2O_5 mixed oxides have already been characterized (14). These mixed oxides performances have been measured with the same techniques and under the same experimental conditions as described here for Ta-PILCs.

One of the main features underlined by probe molecules adsorption and catalytic testing is the acid site generation in silicon–tantalum mixed oxides compared to pure tantalum or silicon oxides. Besides, as a consequence of the Si–O–Ta bond formation, the nature (strength) of the Lewis acid sites present in the mixed oxides (LPy 8a = 1614 cm^{-1} at 200°C) differs from the one observed upon the starting materials: Ta_2O_5 (LPy 8a = 1611 cm^{-1}) or SiO_2 (no LPy 8a band is observed at this temperature). Otherwise, the formation of this Si–O–Ta bond has as a consequence, in agreement with Tanabe's theory (10), the creation of new Brønsted acid

sites. Indeed, hydroxyl groups acidic enough to protonice the pyridine (BPy 8a = 1545 cm^{-1}), absent on the starting materials, are observed on mixed oxides. Moreover, the creation of new Brønsted acid sites has been confirmed by the increase of 1-butene isomerised into 2-butenes over mixed oxides (68%) compared to tantalum oxide (38%).

The comparative analysis of tantalum pillared clays and silicon–tantalum mixed oxides indicates that these solids possess similar acidic properties and catalytic performances. Indeed, probe molecules adsorption and catalytic testing show an acid site generation in both Ta-PILC and Ta_2O_5–SiO_2 mixed oxides compared to their starting materials. Besides, the other two main features associated with the Si–O–Ta bond formation within mixed oxides, (i) change of Lewis acid sites nature and (ii) creation of new Brønsted acid sites, are also observed for Ta-PILCs.

The available experimental data about 1-butanol dehydration over aluminium and titanium pillared montmorillonites seem to confirm the generation within PILCs of the acidic centers of the same nature as observed for the mixed oxides. Indeed, the percentage of 1-butene isomerized on Al-PILCs, characterized by Shen *et al.* (31), is identical, 70%, to that of SiO_2–Al_2O_3 ($3 < \%\ Al_2O_3 < 50\%$) tested by Berteau *et al.* (17). On the other hand, these performances greatly differ from Al_2O_3 or SiO_2 which under the same reaction conditions are not able to isomerize 1-butene. In the same way, whereas titanium oxide isomerizes 33% of 1-butene obtained from 1-butanol, for the Ti-PILC synthesized and characterized by Castillo Paredes (32), this percentage is 67%. The comparison of the experimental data mentioned above is easily done as all have been obtained in our laboratory under the same experimental conditions.

CONCLUSIONS

Probe molecule adsorption and catalytic testing show an acid site generation in Ta-PILCs compared to starting materials. Both Brønsted and Lewis acid sites are present on tantalum pillared montmorillonites surface. The intercalation of tantalum pillars in the interlayer space of the montmorillonite generates Brønsted acid sites.

The incorporation of the tantalum oxide between the montmorillonite sheets produces, within Ta-PILCs, acidic centers of the same nature as those observed for the silicon-tantalum mixed oxides. Therefore, the existence in the Ta-PILC matrix of Si–O–Ta bonds, "cross-linking" pillars and the montmorillonite sheets, similar to those present on mixed oxides, seems to be confirmed. The acidity improvement observed for Ta-PILCs compared with the starting materials has its origin on the acid sites carried in the linkage of pillars and clay.

The acidity measurements indicate that Ta-PILC performances are comparable to the Zr, Al, or Ti pillared clays, which are the most studied at the moment due to their potential industrial applications. Moreover, the great advantage of these new pillared clays compared to the tested Ti or Al-PILCs is the production of butenes with 100% selectivity. The absence of butyraldehyde and dibutylether in the product stream is probably due to the lack of basic sites.

ACKNOWLEDGMENTS

We thank "Eusko Jaurlaritza" (Grant BFI90.61 Modalidad AK) and the "Service de la Programmation de la Politique Scientifique," Belgium, for their financial support.

REFERENCES

1. Laszlo, P., *Science* **235**, 1474 (1987).
2. "Zeolites and Related Microporous Meterials: State of the Art 1994" (J. Weitkamp, H. G. Karge, H. Pfeifer, and W. Hölderich, Eds.), *Stud. Surf. Sci. Catal.*, Vol. 84, part A. Elsevier, Amsterdam, 1994.
3. Venuto, P. B., *Microporous Mater.* **2**, 297 (1994).
4. Viswanathan, B., and Pillai, C. N., "Recent Developments in Catalysis: Theory and Practice." Editions Technip, 1992.
5. Frenkel, M., *Clays Clay Miner.* **22**, 435 (1974).
6. Tichit, D., Mountassir, Z., Figueras, F., and Auroux, A., *in* "Preparation of Heterogeneous Catalysts" (G. Poncelet, P. A. Jacobs, P. Grange, and B. Delmon, Eds.), *Stud. Surf. Sci. Catal.*, Vol. 63, p. 345. Elsevier, Amsterdam, 1990.
7. Kikuchi, E., and Matsuda, T., *Catal. Today* **2**, 297 (1988).
8. Jones, W., *Catal. Today* **2**, 357 (1988).
9. Figueras, F., *Catal. Rev. Sci. Eng.* **30**, 457 (1988).
10. Tanabe, K., Misono, M., Ono, Y., and Hattori, H., *in* "New Solid Acids and Bases. Their Catalytic Properties" (B. Delmon and J. T. Yates, Eds.), *Stud. Surf. Sci. Catal.*, Vol. 51, p. 128. Elsevier, New York, 1989.
11. Thomas, J. M., and Theocharis, C. R., "Perspectives in Catalysis" (J. M. Thomas and K. I. Zamaraev, Eds.). Blackwell, Oxford, 1992.
12. Farfan-Torres, E. M., Sham, E., and Grange, P., *Catal. Today* **15**, 515 (1992).
13. Guiu, G., Gil, A., Montes, M., and Grange, P., *J. Catal.*, **168**, 450 (1997).
14. Guiu, G., and Grange, P., *Bull. Chem. Soc. Jpn.* **67**, 2716 (1994).
15. Guiu, G., and Grange, P., *J. Catal.* **156**, 132 (1995).
16. Forni, L., *Catal. Rev.* **8**, 65 (1963).
17. Berteau, P., Delmon, B., Dallons, J. L., and van Gysel, A., *Appl. Catal.* **70**, 307 (1991).
18. Laitinen, H. A., and Harris, W. E., "Chemical Analysis. An Advanced Text and Reference." McGraw-Hill, New York, 1982.
19. Occelli, M. L., *J. Mol. Catal.* **35**, 377 (1986).
20. Auer, H., and Hofmann, H., *Appl. Catal. A: Gen.* **97**, 23 (1993).
21. Del Castillo, H. L., and Grange, P., *Appl. Catal.* **103**, 23 (1993).
22. Bodoardo, S., Figueras, F., and Garrone, E., *J. Catal.* **147**, 223 (1994).
23. Vinek, H., *Zit. für Phys. Chem. Neue Folge* **121**, 249 (1980).
24. Itoh, M., Hattori, H., and Tanabe, K., *J. Catal.* **35**, 225 (1974).
25. Nakano, Y., Iizuka, T., Hattori, T., and Tanabe, K., *J. Catal.* **57**, 1 (1979).
26. Goldwasser, J., Engelhardt, J., and Hall, W. K., *J. Catal.* **71**, 381 (1981).
27. Patrono, P., La Ginestra, A., Ramis, G., and Busca, G., *Appl. Catal.* **107**, 249 (1994).
28. Chang, C. C., and Kokes, R. J., *J. Phys. Chem.* **77**, 1957 (1973).
29. Fukuda, Y., Hattori, H., and Tanabe, K., *Bull. Chem. Soc. Jpn.* **51**, 3150 (1978).
30. Fripiat, J. J., *Catal. Today* **2**, 281 (1988).
31. Shen, Y. F., Ko, A. N., and Grange, P., *Appl. Catal.* **67**, 93 (1990).
32. Castillo Paredes, H. L., "Mémoire de Licence en Science Naturelles Appliquées." Université Catholique de Louvain, Louvain la Neuve, 1990.